Supporting Information

Ultra-Bright Stretchable Electroluminescent Devices at Low Driving Fields Enabled by a High-Permittivity Elastomer

Zupeng Liu,[a] Xia Lei,[a] Di Tan,[b] Zhao Liu,[c] Zugan Zou,[a] Yujue Yang,[a]* Titao Jing[a]*

[a] School of Chemical Engineering and Technology, Southern Marine Science and Engineering Guangdong Laboratory (Zhuhai), Sun Yat-sen University, Zhuhai 519082, China;

[b] Department of Mathematics and Information Technology, The Education University of Hong Kong, 999077, Hong Kong, China;

[c] Centre for Quantum Technology Theory, Swinburne University of Technology, Melbourne 3122, Australia;

* Corresponding author, E-mail: yujue1031.yang@connect.polyu.hk, jingtt@mail.sysu.edu.cn,

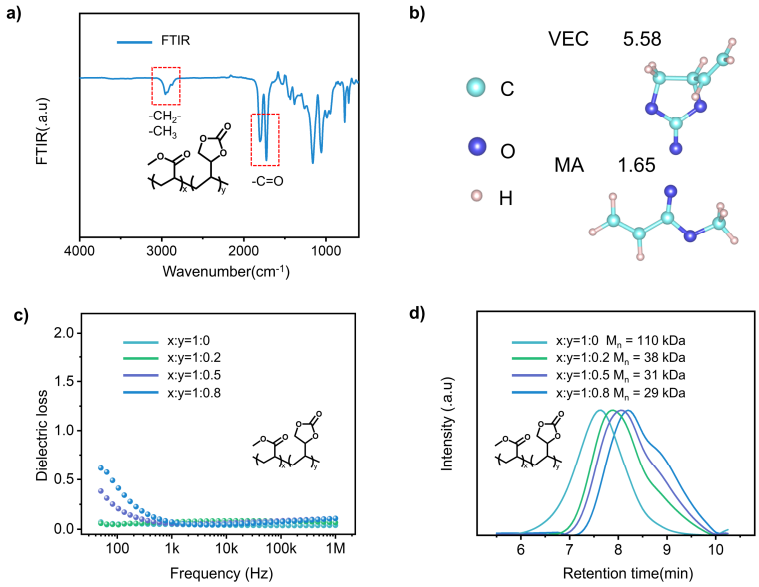


Figure S1. **a)** FTIR spectrum of high-permittivity PMV. **b)** Dipole moments of monomers for PMV, calculated via Density Functional Theory (DFT). **c)** Dielectric loss of PMV and other commonly used matrices for stretchable ACEL devices. **d)** Number-average molecular weights, M_n, of PMV with different structural unit ratios, measured via Gel Permeation Chromatography.

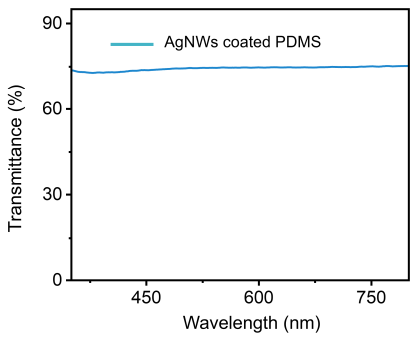


Figure S2. Optical transmittance AgNWs coated PDMS electrode.

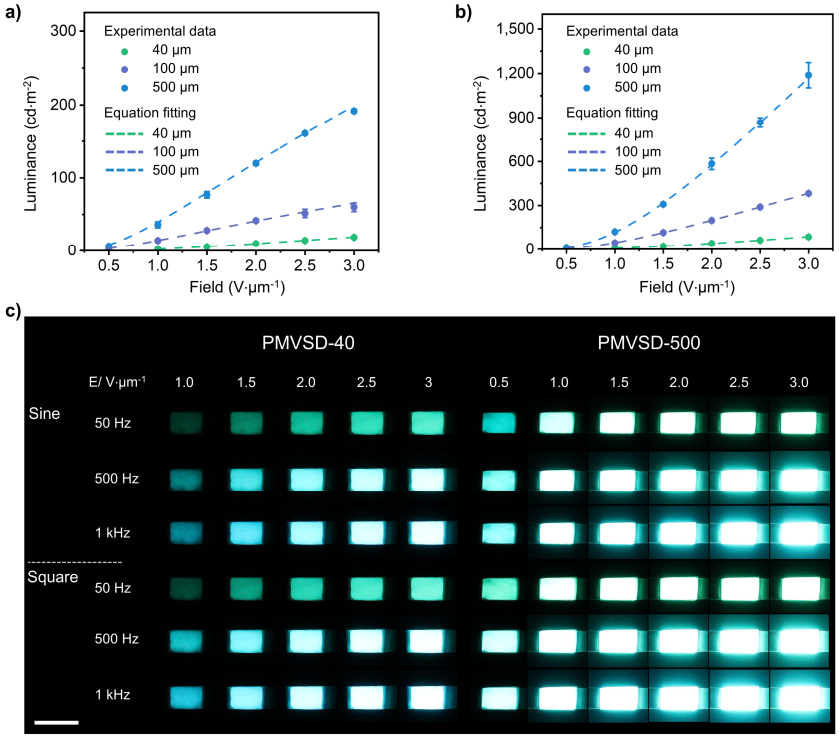


Figure S3. The luminance of PMVSD with different thicknesses at different square electric fields, **a)** 50 Hz, and **b)** 500 Hz. The dashed lines are the fitting lines. **c)** Digital photos of PMVSD-40 and PMVSD-500 at different electric fields. Scale bar: 2cm.

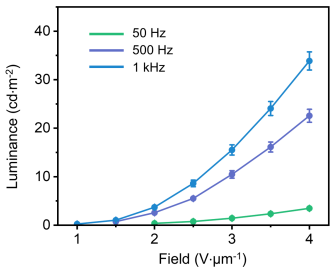


Figure S4. Luminance of PDMS-based devices under different electric fields.

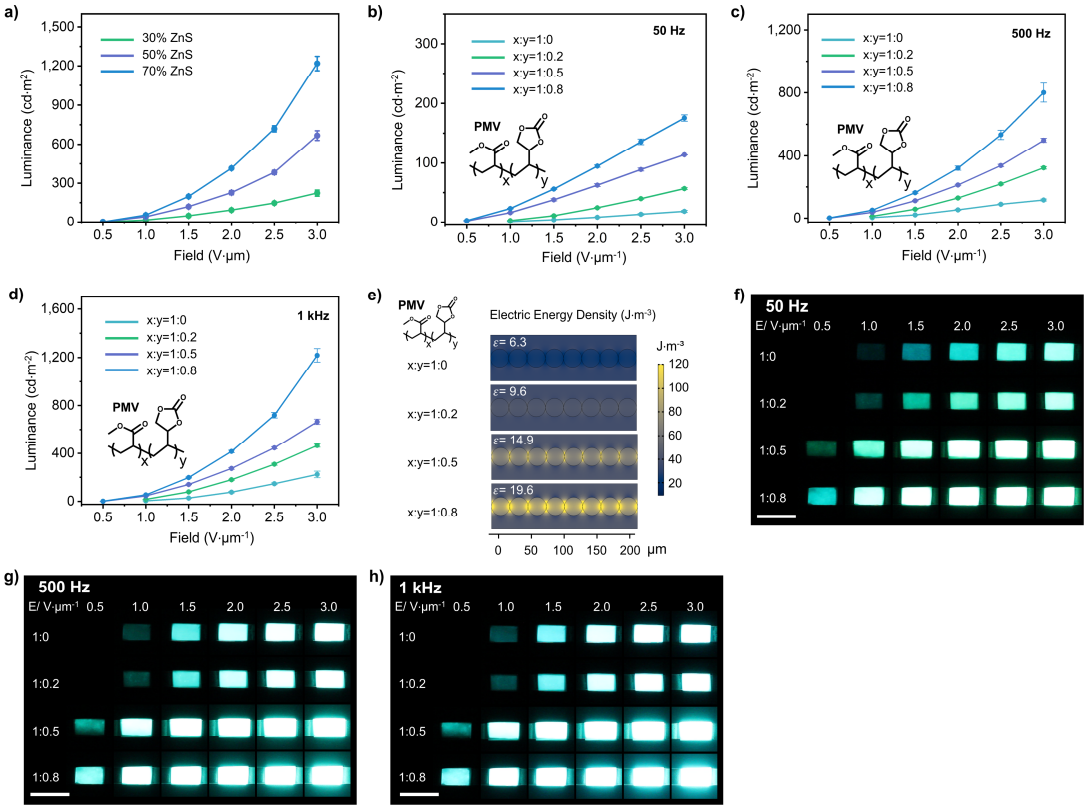


Figure S5. **a)** Influence of ZnS particle content in PMV on the luminance of PMVSD-100 (measured at 1 kHz). Influence of elastomer structural unit ratios on the luminance of PMVSD at **b)** 50 Hz, **c)** 500 Hz, and **d)** 1 kHz. **e)** COMSOL simulations of ZnS particle-doped PMV with different structural unit ratios. Digital photos of PMVSD with different structural unit ratios **f)** 50 Hz, **g)** 500 Hz, and **h)** 1 kHz. Scale bars: 2cm.

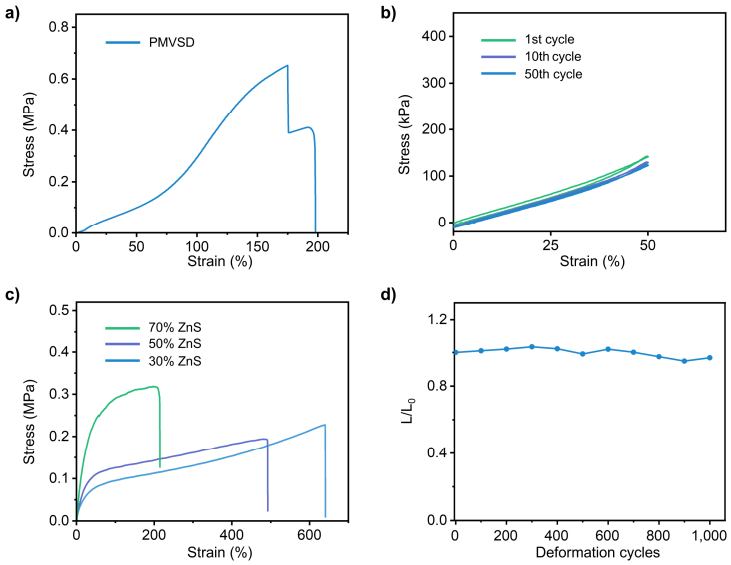


Figure S6. **a)** The stress-strain curve of PMVSD. **b)** Cyclic stress−strain curves of PMVSD for 50 cycles at 50% strain. **c)** Influence of ZnS particle content on the stretchability of ZnS-doped PMV, the emitting layer. **d)** Relative luminance L/L_0 of PMVSD-100 for different deformation cycles, including twisting, bending and stretching.

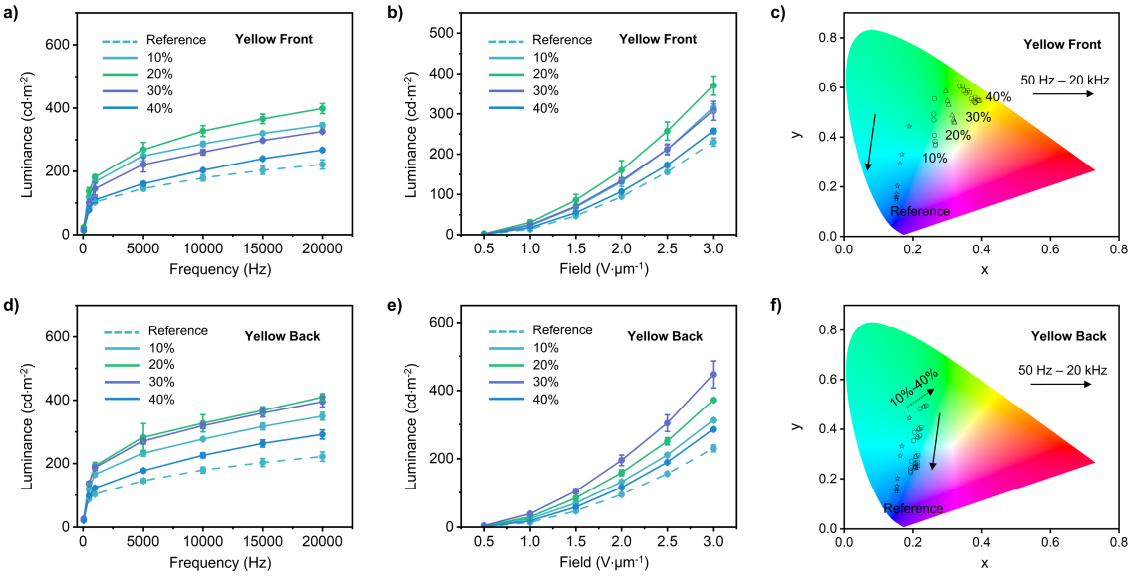


Figure S7. Effects of fluorescent particle (YAG:Ce) content on PMVSD-100 with yellow Electrodes: **a)** front-side luminance under different frequencies, **b)** front-side luminance under different electric fields, **c)** front-side CIE coordinates, **d)** back-side luminance under different frequencies, **e)** back-side luminance under different electric fields, and **f)** back-side CIE coordinates.

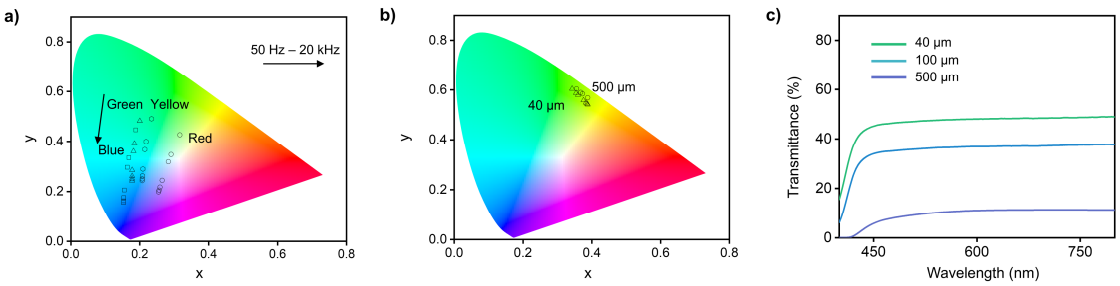


Figure S8. **a)** The CIE coordinates in back sides of PMVSD with fluorescent electrodes over a driving frequency range of 50 Hz–20 kHz. **b)** CIE coordinates of the front side of PMVSD with different emitting layers. **c)** Transmittance of emitting layers with different thicknesses.

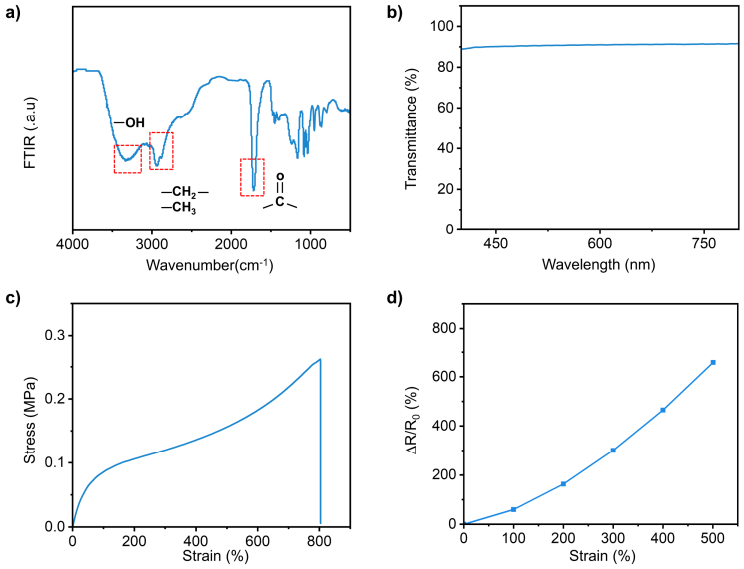


Figure S9. **a)** FTIR spectrum, **b)** optical transmittance, and **c)** stress-strain curve of gel electrodes, and **d)** $\Delta R/R_0$ at different strains.

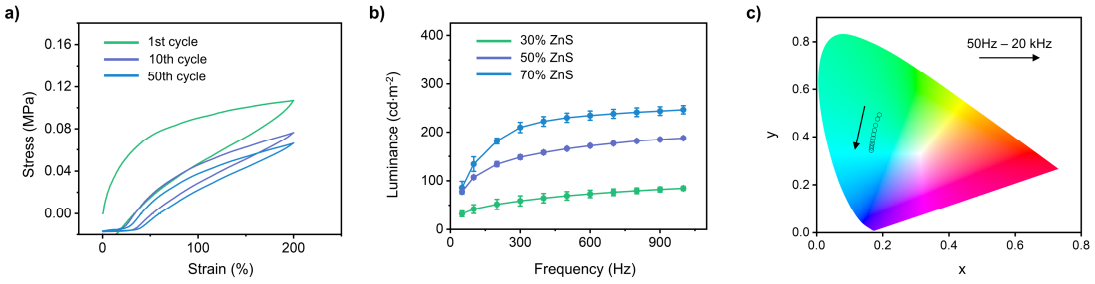


Figure S10. **a)** Cyclic stress−strain curves of gel electrode-based PMVSD over 50 cycles at 200% strain. **b)** Luminance of gel electrode-based PMVSD with different ZnS particle contents under varying frequencies. **c)** CIE coordinates of gel electrode-based PMVSD under different frequencies.

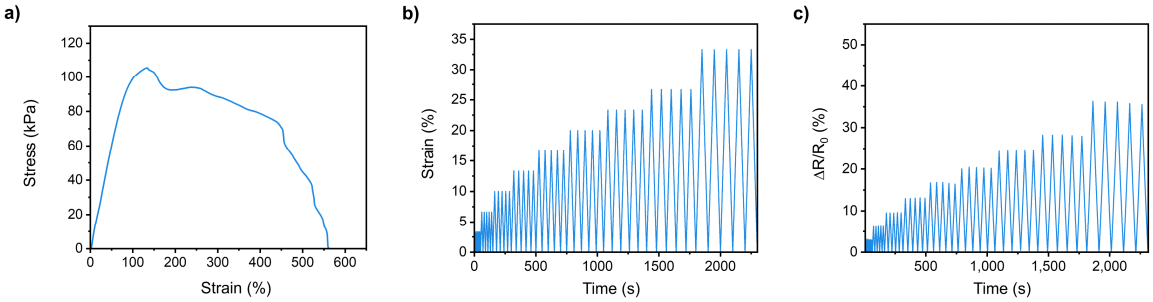


Figure S11. **a)** Stress-strain curve of sensors. 5 cycles of sensors at different **b)** strains and **c)** their corresponding $\Delta R/R_0$.

Table S1. A comparison of PMVSD with reported stretchable ACEL devices based on the applied electric field and their corresponding luminance. Since the cited references lack detailed data and experimental conditions, we focus on core parameters including frequency, electric field and thickness.

Field ($V \cdot \mu m^{-1}$)	0.5	1	1.5	2	2.5	3	4	5	EL phosphor (wt%)	Dielectric matrix	Emission layer thickness(μm)	Frequency
ACEL	Luminance ($cd \cdot m^{-2}$)											
PMVSD-40	NA	5.2	18	36.3	58.2	81.6	NA	NA	70%	PMV	40	1 kHz (sinusoidal)
PMVSD-40	NA	9.16	19.2	57.6	88.8	123.5	NA	NA	70%	PMV	40	1 kHz (square-wave)
PMVSD-100	1	15.9	48.6	99.3	159.8	230.8	NA	NA	70%	PMV	100	1 kHz (sinusoidal)
PMVSD-100	2.8	48.4	132.7	243.7	365.6	517.3	NA	NA	70%	PMV	100	1 kHz (squarc-wavc)
PMVSD-500	1.3	54.2	198	415.3	719.2	1218.7	NA	NA	70%	PMV	500	1 kHz (sinusoidal)
PMVSD-500	9.6	151.2	432.4	871	1548.8	2117.6	NA	NA	70%	PMV	500	1 kHz (square-wave)
Ref.1	15.4	106.1	307.1	556.5	952.2	NA	NA	NA	70%	Dielectric gel	500	1 kHz (square-wave)
Ref.1	22.1	141.6	479.9	1061.4	1823.5	NA	NA	NA	70%	Dielectric gel	800	1 kHz (square-wave)
Ref.2	NA	6.2	NA	66.6	119.5	178.1	320.2	468.4	70%	PVDF-HFP /5 wt% FS300	100	1 kHz (sinusoidal)
Ref.2	NA	10	NA	121.8	221.0	369.4	779.3	823.7	50%	PVDF-HFP /5 wt% FS300	500	1 kHz (sinusoidal)
Ref.2	NA	29	NA	500.4	1459.7	NA	NA	NA	70%	PVDF-HFP /5 wt% FS300	1500	1 kHz (sinusoidal)
Ref.3	NA	~5	~30	~75	~150	~200	319	NA	67%	Ecoflex/Triton X	100	15 kHz (square-wave)
Ref.4	NA	NA	NA	0.4	NA	2.3	11.5	21	37%	$BaTiO_3$-PDMS	33	400 Hz
Ref.5	NA	13.5	NA	63.7	98.9	134	213.6	NA	NA	SEBS	43	20 kHz
Ref.6	NA	3.8	NA	153.2	NA	360.2	771.8	1211.7	50%	TFE-HF-PFPE	560	1 kHz
Ref.7	NA	16.8	NA	127.7	239.0	335.3	579.6	905.9	67%	PVDF-HFP /10 wt% FS300	141	1.5 kHz
Ref.8	NA	NA	NA	NA	18.8	39.2	105.9	NA	40%	PVDF-HFP/TEAc	110	1khz
Ref.9	NA	~3	~10	~20	~30	~40	57.5	~60	75%	PDMS/BTO-La	~60	1 kHz

References

1. Liu Z, Liu Z, Lei X, Yang Y, Jing T. Ultra low-field-emission stretchable electroluminescent devices enabled by a transparent and high-κ dielectric gel. Nature Communications, 16, 11190 (2025)
2. Tan Y J, Godaba H, Chen G, et al. A transparent, self-healing and high-κ dielectric for low-field-emission stretchable optoelectronics. Nature Materials, 19(2), 182-189 (2020).
3. Oh SJ, Choi SE, Woo I, Yoon JU, Bae J, Bae JW. Stretchable Multicolored Electroluminescent Sound Display for Wearable and Interactive Textiles. Advanced Functional Materials, 35(31), 2420432 (2025).
4. Stauffer, F. & Tybrandt, K. Bright Stretchable Alternating Current Electroluminescent Displays Based on High Permittivity Composites. Advanced Materials, 28, 7200–7203 (2016).
5. Chun F, Zhang B, Gao Y, et al. Multicolour stretchable perovskite electroluminescent devices for user-interactive displays. Nature Photonics 18, 856–863 (2024).
6. Liu Y, Sun L, Feng W, et al. A Stable, Self-Healable, and Stretchable Dielectric Polymer for Electroluminescent Device Working Underwater. Advanced Functional Materials, 34, 2402453 (2024).
7. Fu X, Wan G, Guo H, et al. Self-healing actuatable electroluminescent fibres. Nature Communications, 15, 10498 (2024).
8. Zhang P, Lei I M, Chen G, et al. Integrated 3D printing of flexible electroluminescent devices and soft robots. Nature Communications, 13(1), 4775 (2022).
9. Shanker R, et al. Solution‐Processable, High‐Performance Flexible Electroluminescent Devices Based on High‐k Nanodielectrics. Advanced Functional Materials, 29(39), 1904377 (2019).